frontiers in Built Environment

ORIGINAL RESEARCH
published: 17 May 2021
doi: 10.3389/fbuil.2021.665549

Impact of Silica Nanoparticles on the Durability of fly Ash Concrete

D. Ali[1,2], *U. Sharma*[1], *R. Singh*[3] *and L. P. Singh*[1]*

[1]CSIR- Central Building Research Institute, Roorkee, India, [2]Uttarakhand Technical University, Dehradun, India, [3]D.B.S. (PG) College, Dehradun, India

In the present study, the mechanical and durability properties of silica nanoparticle (SNP)-incorporated fly ash (FA) concrete mix were examined after 365 days of exposure. The dosages of FA replaced by cement in the present study were 30%, 40%, and 50%, while 3% SNPs were added by the weight of cement in the FA incorporated mix. For a comparison of SNPs with silica fume (SF), 6% SF was added (by the weight of cement) and entire casting was performed at a constant water to binder (w/b) ratio of 0.29. The present work is the extension of a previous study wherein durability properties of the same mixes were reported for up to 180 days of exposure. Compressive strength results show that in the presence of SNPs, the enhancement in compressive strength was in the range of 10–14%, while, in presence of SF, 8–10% of the enhancement was observed as compared to control. However, exposed samples in a carbonation environment showed that the compressive strength of the control and SF incorporated mix increased, while SNP-incorporated samples showed negligible enhancement. Further, sulphate exposed mix show that compressive strength decreases, however, the SNP-incorporated mix showed the lowest reduction compared to other mixes. Therefore, the study shows that the SNP-incorporated mix has higher mechanical properties and more durability compared to other mixes in a severe environment.

Keywords: silica nanoparticles, fly ash, carbonation, sulphate, CH and C-S-H

OPEN ACCESS

Edited by:
Wengui Li,
University of Technology Sydney, Australia

Reviewed by:
Xiaojian Gao,
Harbin Institute of Technology, China
Bin Lei,
Nanchang University, China
Xuemei Liu,
The University of Melbourne, Australia
Guangcheng Long,
Central South University, China

***Correspondence:**
L. P. Singh
lpsingh@cbri.res.in

Specialty section:
This article was submitted to Sustainable Design and Construction, a section of the journal Frontiers in Built Environment

Received: *08 February 2021*
Accepted: *15 April 2021*
Published: *17 May 2021*

Citation:
Ali D, Sharma U, Singh R and Singh LP (2021) Impact of Silica Nanoparticles on the Durability of fly Ash Concrete. Front. Built Environ. 7:665549. doi: 10.3389/fbuil.2021.665549

INTRODUCTION

Extensive utilization of concrete by the construction industries has led to the enormous consumption of cement, and it is thus necessary to preserve the buildings in their original forms for a long time with sustainable material. Therefore, researchers have been developing sustainable concrete using less energy and supplementary cementitious materials to reduce the carbon footprint of cement (Guterres, 2017). Different supplementary cementitious materials, such as fly ash (FA), ground granulated blast furnace slag, calcined clay, etc., were used as replacements for cement. Mo et al., 2021 investigated the microscopic performances of metakaolin (MK) containing a UHPC matrix using steam curing. They have reported that MK reaction kinetics increased with higher curing temperature; however, cement hydration rate reduced. Zhang et al., 2021 have investigated the role of steam curing in the performance of PC incorporating self-ignited coal gangue (CG) particles. They have reported that steam curing can significantly activate the pozzolanic reaction of the CG particle and alleviate the negative impact arising from CG addition. It is well known that FA is generated as waste from thermal power stations. FA has uses in different sectors, such as cement/concrete production (Malhotra, 1990; Teixeira et al., 2016), soil stabilization (Pereira et al., 2009), and Geopolymer concrete (Embong et al., 2016). In cement and concrete, FA improves fresh stage

properties, reduces shrinkage at an early age, and improves durability and mechanical strength at the later stages (Basheer et al., 2001; Sahmaran and Li, 2009; Dananjayan et al., 2016). RameshKumar and Muzammil (2020) investigated the compressive strength of the FA concrete using seawater, and they have reported that FA concrete is more durable in a marine environment compared to a conventional one. McCarthy et al., 2005 reported that FA can be replaced with cement up to 45%; however, early age strength was reduced compared to the control. However, low early age strength in the cementitious system is the major drawback of an FA-incorporated cementitious system (Lam et al., 2000; Sakai et al., 2005). To address this problem, concrete technology extensively uses different additives, such as SF, natural pozzolanas, silica nanoparticles (SNPs), etc. Rattanachu et al. (2020) utilized rice husk ash as a cementitious material and reported that rise husk ash improves the mechanical properties of concrete containing recycled aggregate concrete (RAC) at 60 days of hydration. SNPs accelerate the hydration process by proving additional nucleation sites and densify the microstructure due to the formation of additional calcium silicate hydrate (C-S-H) through a pozzolanic reaction (Sobolev and Shah, 2008; Sanchez and Sobolev, 2010; Hou et al., 2013; Sobolev, 2015).

SNP incorporation into concrete leads to additional hydration product formation, which reduces the capillary porosity of the concrete. This is helpful for the formation of dense microstructures in concrete and strengthening of bonding between aggregate and cement paste, thereby leading to higher mechanical strength and also enhanced durability of concrete (Nili and Ehsani, 2015). Researchers have evaluated the durability properties of SNP-incorporated concrete and have found ~31% reduction in chloride diffusion coefficient with 0.3% dosage of SNPs into the concrete (Du et al., 2014). Shaikh and Supit (2015) have found that the addition of 1% of nano calcium carbonate and 2% dosage of SNPs into the concrete reduces the chloride penetration by ~21 and ~27%, respectively. Kawashima et al. (2013) investigated the effect of SNPs on high volume fly ash (50% replacement). Sharkawi et al. (2018) have described that a mixture of 8% micro silica and 2% SNPs reduces water permeability and chloride ions penetration by ~38 and ~47% respectively. Mukharjee and Barai (2014) have observed that the addition of 3% colloidal SNPs in mortar reduces water absorption by 20%, while Salemi and Behfarnia (2013) have observed a similar reduction in water absorption with the addition of 5% SNPs in concrete. Heikal et al. (2020) investigated the impact of SNPs on the physicochemical and microscopic characteristics of composite cements containing 40–60 mass% FA and/or granulated-slag (GS). They have reported that SNPs have a positive effect on the behavior of composite cement pastes, it diminished the setting times and improved the compressive strength and gel/space ratio. Singh et al. (2016) performed a systematic study on tricalcium silicate, cement paste, mortar, and concrete and reported that the optimized dosages of SNPs in cementitious systems are 3% at w/b ratio 0.4. Further, Palla et al., 2017 investigate the effect of SNPs on high volume fly ash concrete, wherein they have reported that the optimized dosages of SNPs with a w/b ratio 0.3 is 3%.

TABLE 1 | Physio-chemical properties of cement, fly ash, SNPs, and silica fume.

Property	Cement	Fly ash	Silica fume	SNPs
Particles Size	50–90 μm	25–30 μm	<1 μm	40–70 nm
Appearance	Powder form	Powder form	Powder form	Powder form
Colors	Gray	Light Gray	Light Gray	White
Density (g/cm^3)	3.15	2.25	1.86	1.40
LOI (%)	0.50	1.33	1.89	-
CaO (%)	63.38	1.61	0.28	-
SiO_2 (%)	19.00	55.27	96.03	99.80
Al_2O_3 (%)	3.90	26.69	0.43	-
MgO (%)	3.31	0.39	0.63	-
Fe_2O_3 (%)	4.36	8.14	0.99	-
SO_3 (%)	3.14	0.25	0.30	-
Alkalis (%)	2.24	1.89	1.03	-

Despite the fact that the use of FA in concrete is well established, the use of high volume fly ash remains, however, unresolved due to problems such as high carbonation, sulphate attack, and increased shrinkage. Therefore, Singh et al. (2019) performed a durability study, wherein durability of FA concrete was reported up to 180 days. The present study focus on the mechanical properties of exposed and non-exposed SNPs and SF incorporated FA concrete samples.

EXPERIMENTAL DETAILS

Materials and Methods

For the present study, we looked at ordinary Portland cement (OPC-43 grade) with Blain fineness of 390 m^2/kg confirm IS 8112:1989 (IS-8112, 1989). FA was used in the present study and was of class F type with a fineness 410 m^2/kg confirming IS 3812 (part 2): 2003 (IS-3812, 2013). SNPs were synthesized in a laboratory using water glass (sodium silicate solution) as a precursor, as reported elsewhere in further detail (Singh et al., 2015). The synthesized SNPs were amorphous and well dispersed, having a specific surface area of 116 m^2/g. SF was procured from Elkem Ltd. and had a particle size <1 μm (Holland, 2005). The physiochemical properties of cement, FA, SNPs, and SF are given in **Table 1**.

For casting the concrete specimens, river sand with a fineness modulus of 2.72 and specific gravity 2.64 was used as fine aggregates. Meanwhile, angular crushed siliceous aggregates of a maximum size ~12.5 mm were used as coarse aggregates, and they had a specific gravity of 2.63 and fineness modulus 7.49. The aggregates were found to be satisfying the specifications of IS:383: 1970 (IS-383, 1970). Particle size distribution curve of fine sand and coarse aggregates are presented in **Figures 1**,**2**. Fourth-generation superplasticizer (SP) polycarboxylic ether (Glenium 51 of BASF, India) was used to achieve the desired workability of concrete confirming to IS 9130:1999 (IS-9130-1999IS-9130-1999).

Mix Proportion and Casting

The dosages of FA replacement used in the present study were 30%, 40%, and 50% by weight of cement, and the dosages of SNPs and SF added in FA concrete were 3 and 6% by weight of cement,

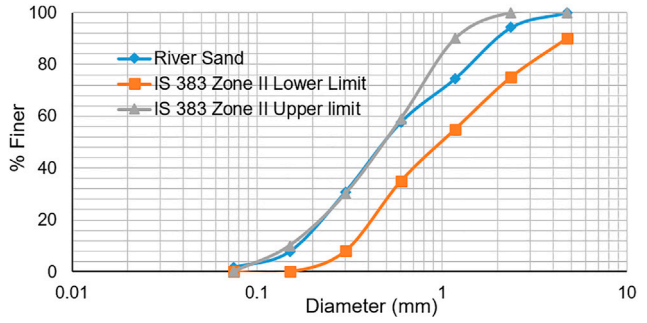

FIGURE 1 | Particle size distribution curve of fine sand.

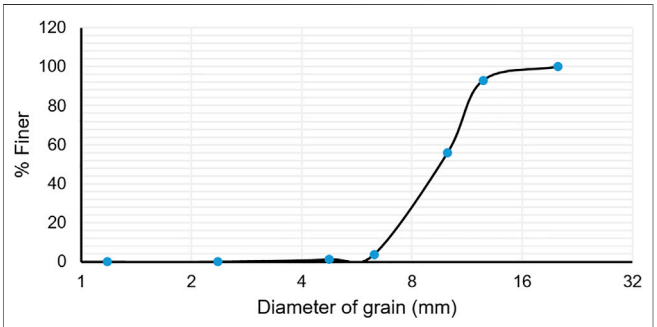

FIGURE 2 | Particle size distribution curve of coarse aggregates.

respectively. Details of the mix design used for the present study are given in **Table 2**. The SNPs and SF were first mixed with cement in dry form, and this mix was used as a binder with FA for the concrete casting with a water-to-binder ratio (w/b) of 0.29 for the entire casting. The dosages of SNPs and SF were optimized on the basis of previous study and literature (Mazloom et al., 2004; Singh et al., 2016; Palla et al., 2017). The SF and SNPs were mixed with cement first in dry form, and then this cement (SNPs and SF incorporated) was used for concrete casting. The FA concrete casting was carried out as per IS 10086:1982 (IS-10086, 1982). Casted samples were demoulded after 24 h and cured in tap water at room temperature for 28 days as per IS 516:1959 (IS-516, 1959).

Compressive, Split Tensile and Flexural Strength Testing

The compressive strength tests of concrete samples were carried out on 100 × 100 × 100 mm cubes as per IS 516:1959 (IS-456, 2000). The split tensile strength test was performed on 100 × 200 mm cylinders according to ASTM C 496–11 (ASTM C496-11, 2003) and the flexural strength test performed on 100 × 100 × 500 mm prism samples as per IS 516: 1959 (IS-456, 2000). The split tensile strength is also estimated from the compressive strength of concrete by using standards like ACI 318–14 (ACI Committee 318, 2014) and Chinese Code GB 50010–2002 using the following equation (Xiao et al., 2007):

$$f_{sp} = 0.49 f_{cu}^{0.50} \tag{1}$$

$$f_{sp} = 0.19 f_{cu}^{0.75} \tag{2}$$

The compressive strength of concrete is also frequently used to calculate the flexural strength of concrete and is given by the following equation:

$$f_f = 0.81\sqrt{f_{cu}} \tag{3}$$

$$f_f = 0.54\sqrt{f_{cu}} \tag{4}$$

Porosity

The porosity of exposed (in carbonation and sulphate environment) and non-exposed concrete samples were evaluated using ASTM C642 (ASTM-C642, 2015). The test was carried out on exposed samples (carbonation and sulphate) having size 100 × 200 mm cylinders after 365 days. The porosity was determined by using the following equation (Chindaprasirt and Rukzon, 2008):

$$p = \frac{W_a - W_d}{W_a - W_w} \tag{5}$$

where.

P is the vacuum-saturated porosity.

W_a is the weight of the sample when air saturated (gm).

W_d is the weight of the sample after oven drying (gm).

W_w is the sample weight in water (gm).

Carbonation Depth

The carbonation depth was investigated as per RILEM CPC-18 (Gehlen, 2011) after 365 days of exposure. The exposure condition for carbonation was 2% CO_2, 65% RH and 20°C. From exposed samples of concrete, a slice of size 50 × 100 × 100 mm cut from the prism, the carbonation depth was determined by using phenolphthalein solution.

Determination of Diffusion Coefficient and Carbonation Depth by Model

The determination of D_{CO_2} in carbonated samples of SNPs, SF incorporated and control specimens were carried out using the following equation (Ta et al., 2016).

$$D_{CO_2} = D_{CO2}^{28} \times f(RH) \times f(T) \times f\left(\frac{S+G}{C}\right) \times f\left(\varphi, \frac{W}{C}, FA\right) \times f(t_c) \tag{6}$$

Where, function D_{CO2}^{28} is the CO_2 diffusion coefficient, which depends on the compressive strength of concrete, function $f(RH)$ is external relative humidity. The function $f(T)$ is ambient temperature $f(S+G/C)$ is the function of aggregate and cement ratio $f(\varphi, W/C, FA)$ is the function of porosity, w/b ratio and replacement of FA by cement content, and $f(t_c)$ is the empirical correction term in Fib's model. The carbonation depth of concrete with 3% SNPs and 6% SF incorporated specimens was determined using the model as per equation (Demis et al., 2014).

$$X_{Co2} = \sqrt{\frac{2D_{Co2}(CO2/100)t}{0.33CH + 0.214CSH}} \tag{7}$$

TABLE 2 | M60 mix proportion for fly ash concrete mixes.

Mix	Material (kg/m^3)								
	Cement	FA	Ca	SP	Fly ash	SNPs	SF	W/b	C. S. (MPa) at 28 days
30FA	329	676	1278	1.31	141	-	-	0.29	45.2
30FA6SF	329	676	1278	1.64	141	-	19.74	0.29	52.7
30FA3SNPs	329	676	1278	1.64	141	9.87	-	0.29	60.3
40FA	282	676	1278	0.98	188	-	-	0.29	38.6
40FA6SF	282	676	1278	1.27	188	-	16.92	0.29	45.7
40FA3SNPs	282	676	1278	1.27	188	8.46	-	0.29	47.4
50FA	235	676	1278	0.70	235	-	-	0.29	32.5
50FA6SF	235	676	1278	0.94	235	-	14.10	0.29	40.2
50FA3SNPs	235	676	1278	0.94	235	7.05	-	0.29	41.7

Here, X_{Co2} is the carbonation depth at time t, CO_2 is the carbon dioxide content (%) at the surface of concrete, CH and C-S-H are the calcium hydroxide and calcium silicate hydrate content in fly ash concrete volume (kg/m^3), D_{CO2} is the diffusion coefficient of CO_2 in fly ash concrete specimens.

Sulphate Attack

The sulphate attack was investigated as per ASTM C1012 (El-Hachem et al., 2012) after 365 days of exposure. The exposure conditions for the sulphate attack were 5% solution of magnesium sulphate maintained at a pH between 6–8 at room temperature. For the determination of sulphate ion concentration in concrete specimens, a powder sample was taken from the exposed samples and determined through chemical analysis as per IS 4032 (IS-4032, 1985).

Characterization Techniques

The compressive, tensile, and flexural strength test was carried out using universal Testing Machine (UTM) (make: Shimadzu, model: UH-1000knI) of capacity 1000 KN at loading rate 0.5 mm/min was used with ±1% potential error. XRD pattern was composed at an X-ray diffractometer (make: Rigaku; model: DMax-2200). Concrete powder samples were examined at 3°/min from 5° to 80° (2Theta) with CuKα radiation produced at 40 mA and 20 kV for the identity of hydration products. Thermogravimetric analysis (TGA) (make: Perkin Elmer; model: Diamond) was performed with 0.225 g of concrete powder sample with 10 C/min heating rate from 50 to 1000°C. The precise observation of mass loss over the temperature ranges for the compositional analysis of the concrete sample provides the estimates of the mass fraction of constituents. The microstructure analysis of concrete samples was observed by Field Emission Scanning Electron Microscope (FESEM) (make: TESCAN; model: MIRA 3).

RESULTS AND DISCUSSION

Compressive Strength

Table 3 represents the effect of SNPs or SF on compressive strength of exposed (carbonation and sulphate environment) and non-exposed FA concrete specimens after 365 days of hydration. The results reveal that exposed specimens in the carbonation environment show higher compressive strength as compare to non-exposed specimens due to the formation of calcite. However, SNPs incorporated 30FA concrete specimens exhibit negligible enhancement in compressive strength showing that in presence of SNPs, the carbonation rate of concrete decreases significantly. While in the case of control specimens, the strength enhancement was around 7% and in SF incorporated specimens the strength enhancement was ~4%. Furthermore, 40 FA and 50 FA concrete specimens exhibit higher compressive strength enhancement as compare to 30 FA specimens, showing more carbonation as the porosity increases with the higher dosages of FA, and, thus, accelerated carbonation occurred. Concrete samples exposed in sulphate solution show strength reduction since, during the sulphate attack, sulphate ions react with the CH and AFm phases, which leads to the formation of ettringite and gypsum, resulting in expending in pressure and cracks. Furthermore, during the sulphate attack, brucite also formed, and its low solubility reduces the alkalinity of concrete and low alkalinity lead to the deterioration of the C-S-H (Neville, 2011). Reduction in strength due to sulphate was also reported by Taha, 2019. Further, the results show that in presence of SNPs, 11% reduction was observed, whereas, SF and control samples show ~13 and ~21%, respectively, after 365 days of exposure. SNP-incorporated specimens show low porosity due to their additional hydration products formation; because of this, sulphate ions and CO_2 molecules cannot penetrate the concrete through the pores

TABLE 3 | The compressive strength of carbonation, sulphate exposed and non-exposed 30%, 40%, and 50% fly ash containing 3% SNPs and 6% SF incorporated concrete samples after 365 days of exposure.

Mix	Compressive strength (MPa)		
	Non-exposed	Carbonation	Sulphate exposed
30FA	66.6	71.3	52.3
30FA6SF	72.7	75.6	63.1
30FA3SNPs	73.4	73.8	65.2
40FA	53.5	61.8	42.4
40FA6SF	59.2	67.3	45.9
40FA3SNPs	61.3	65.4	49.1
50FA	51.8	60.6	37.3
50FA6SF	56.4	65.2	43.2
50FA3SNPs	58.6	65.6	45.4

TABLE 4 | The split tensile and flexural strength of sulphate exposed 30%, 40%, and 50% fly ash containing 3% SNPs and 6% SF incorporated concrete samples compared with standard model strength after 365 days exposure.

Mix.	Sulphate exposed							
	Split tensile strength (MPa)				Flexural strength (MPa)			
	f_{sp}	ACI (f_{sp})	GB (f_{sp})	R2	f_f	ACI (f_f)	CEB (f_f)	R2
30FA	3.5	3.7	3.5	0.93±5	5.1	3.9	5.9	0.94±5
30FA6SF	3.9	4.3	3.9		5.6	4.3	6.4	
30FA3SNPs	4.0	4.4	4.0		5.7	4.4	6.5	
40FA	3.2	3.2	3.2		4.6	3.5	5.3	
40FA6SF	3.3	3.3	3.3		4.7	3.7	5.5	
40FA3SNPs	3.4	3.5	3.4		4.9	3.8	5.7	
50FA	3.0	2.9	3.0		4.3	3.3	4.9	
50FA6SF	3.2	3.2	3.2		4.6	3.5	5.3	
50FA3SNPs	3.3	3.3	3.3		4.7	3.6	5.5	

TABLE 5 | The split tensile and flexural strength of carbonation exposed 30%, 40%, and 50% fly ash containing 3% SNPs and 6% SF incorporated concrete samples compared with standard model strength after 365 days of exposure.

Mix	Carbonation exposed							
	Tensile strength (MPa)				Flexural strength (MPa)			
	f_{sp}	ACI (f_{sp})	GB (f_{sp})	R^2	f_f	ACI (f_f)	CEB (f_f)	R^2
30FA	5.5	4.5	4.0	0.93 ± 5	7.9	4.4	6.6	0.94 ± 5
30FA6SF	5.8	4.9	4.3		8.3	4.7	7.0	
30FA3SNPs	5.4	4.8	4.2		7.7	4.6	7.0	
40FA	6.2	4.1	3.8		8.8	4.2	6.3	
40FA6SF	5.5	4.1	3.8		7.9	4.2	6.3	
40FA3SNPs	4.8	4.1	3.8		6.9	4.2	6.2	
50FA	6.3	1.0	3.7		9.0	4.1	6.1	
50FA6SF	5.8	4.1	C.8		83	4.2	6.2	
50FA3SNPs	5.1	4.0	3.7		7.3	4.1	6.1	

(Hou et al., 2014). SNPs containing 40 and 50% FA concrete specimens also show reduction and enhancement in compressive strength after exposure to sulphate and carbonation. In general, admixture SNPs and SF have accelerated the strength at an early age due to its pozzolanic nature and reactivity but, at later ages, strength enhancement is accountable due to the mortar matrix in concrete, which contains additional hydration products.

Flexural and Split Tensile Strength

Flexural and split tensile strength of non-exposed and exposed (carbonation and sulphate environment) FA concrete specimens were determined experimentally and theoretically after 365 days of hydration. **Table 4 Table 5** show the theoretical and experimental results of split and tensile strength of concrete specimens of the mixes and the results reveal that the theoretically evaluate values are in linear relation with the experimental value by a determination coefficient of 93 ± 5. Further, the results reveal that the split tensile strength and flexural strength of SNP-incorporated FA concrete is higher than the control and SF incorporated specimens in the non-exposed condition. However, exposed specimens in the carbonation environment show a different trend, as the control and SF incorporated specimens exhibit higher split and tensile strength than the SNPs incorporated specimens. In the case of sulphate attack, however, SNP-incorporated specimens exhibit higher split tensile and flexural strength than the control and SF incorporated specimens (**Figures 3A–C** and **4A–C**). The reason behind this phenomenon is that, in presence of SNPs, low-density C-S-H converted to high-density C-S-H (Simatupang et al., 2019), which led to the formation of compact microstructure, and, thus, low carbonation and sulphate attack occurred in the SNPs incorporated specimens. The lower effect of both carbonation and sulphate ions confirm that additionally formed hydration products reduce the porosity and significantly improve microstructure (El-Hachem et al., 2012).

Carbonation Depth and Diffusion Coefficients

The carbonation depth of concrete specimens was experimentally determined by using phenolphthalein and theoretically by using a meta model. Further, diffusion coefficient was also determined using compressive strength data at 28 days and other parameters of mix design (**Table 6**) because carbonation is a phenomenon of diffusion of carbon dioxide into concrete, which depends on the

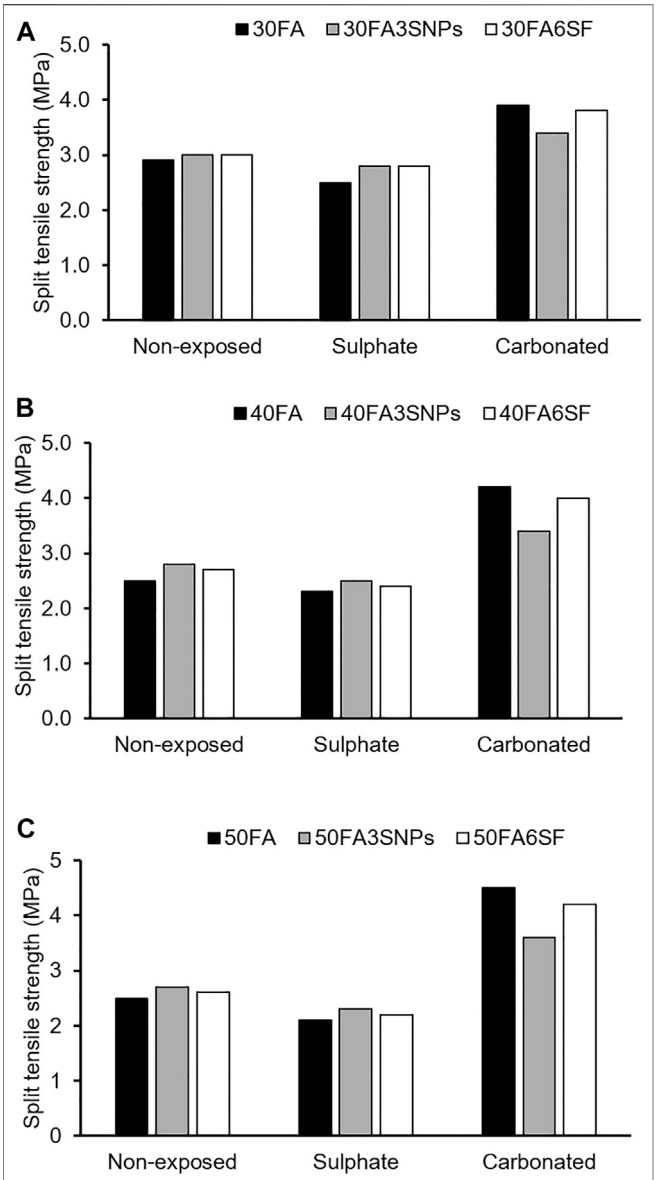

FIGURE 3 | The split tensile strength of exposed and non-exposed **(A)** 30% fly ash containing 3% SNPs and 6% SF **(B)** 40% fly ash containing 3% SNPs and 6% SF and **(C)** 50% fly ash containing 3% SNPs and 6% SF incorporated concrete samples after 365 days of exposure.

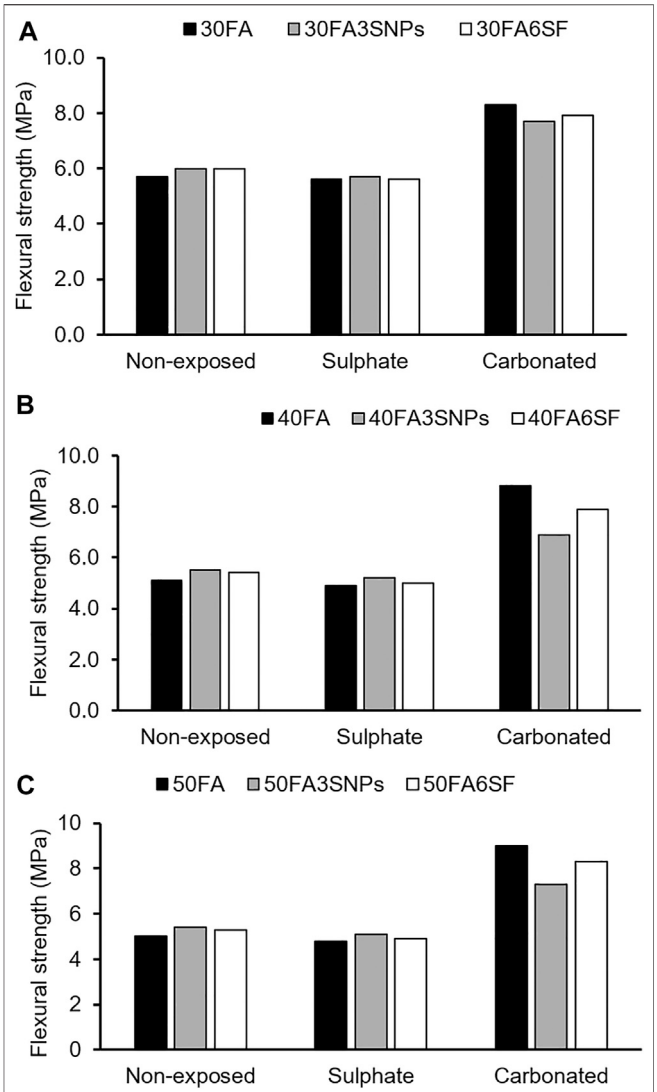

FIGURE 4 | The flexural strength of exposed and non-exposed **(A)** 30% fly ash containing 3% SNPs and 6% SF **(B)** 40% fly ash containing 3% SNPs and 6% SF and **(C)** 50% fly ash containing 3% SNPs and 6% SF incorporated concrete samples after 365 days of exposure.

compressive strength of concrete mix (Ohga and Nagataki, 1989). The results reveal that the carbonation depth increases with the higher dosages of FA due to higher porosity. It was observed that the carbonation depth increased by ~39% in 40FA and ~48% in 50FA than the 30FA concrete mix. In the presence of SNPs, the carbonation depth was decreased by 30–60%, while in presence of SF, the reduction was in the range of 24–28% only. Further, diffusion coefficient results show that SNPs reduce the diffusion coefficient by 95% in the 30FA3SNPs mix, while SF reduces ~66% only. These results reveal that SNPs significantly reduce the carbonation attack, due to the formation of additional C-S-H and dense microstructure.

Sulphate Attack

Sulphate attack on concrete specimens was determined after 365 days of exposure in magnesium sulphate solution and sulphate ion concentration was determined by gravimetric analysis as per IS 4032:1985. Results reveal that the concentration of sulphate ions in concrete specimens increases with the higher dosages of FA, as it was observed that, in 40FA and 50FA mixes, the sulphate ion concentration was above the limit reported in IS 456. In presence of SF, all the mixes have sulphate concentration below the limit except for the 50FA6SF mix, while, in the presence of SNPs, the sulphate ion concentration was below the limit in all the mixes, showing the higher durability of SNPs incorporated concrete specimens in sulphate environment (**Figure 5**). The percentage reductions in sulphate ion concentration in 30FA3SNPs, 40FA3SNPs, and

TABLE 6 | Carbonation depth of 3%SNPs and 6% SF incorporated fly ash concrete specimens with varying the amount of fly ash 30%, 40%, and 50% after 365 days of exposure.

Mix	Diffusion coefficient (x 10^{-8} m^2/s)	Carbonation depth (mm)	
		365 days	
		Exp	Model
30FA	0.60	15.8	11.9
30FA6SF	0.20	11.7	7.2
30FA3SNPs	0.03	6.8	2.3
40FA	2.30	26.1	28.4
40FA6SF	1.70	18.9	23.1
40FA3SNPs	1.50	17.8	20.2
50FA	6.30	30.5	47.7
50FA6SF	4.20	23.2	35.2
50FA3SNPs	4.20	20.7	35.1

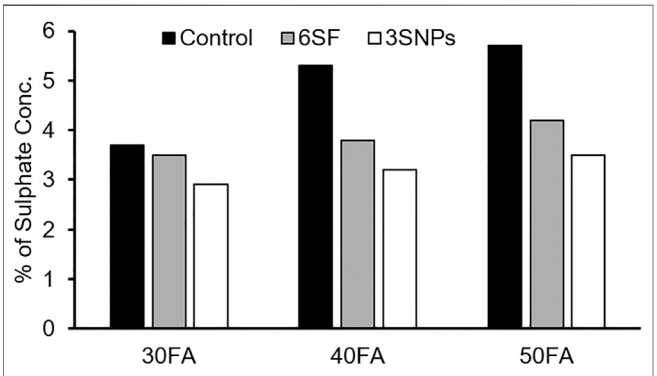

FIGURE 5 | Sulphate ion conc. in fly ash concrete samples having 3% SNPs and 6% SF with varying the amount fly ash 30%, 40%, and 50% after 365 days of exposure.

50FA3SNPs mixes were ~22, ~40, and 39%, respectively, while in the SF-incorporated mixes, i.e., 30FA6SF, 40FA6SF, and 50FA6SF, the percentage reductions observed ere ~5, ~28, and ~26%, respectively.

Effect of Carbonation and Sulphate Attack on Porosity

The porosity of unexposed and exposed concrete specimens was determined by using **equation 5** and the results given in **Figures 6A–C**. Results show that, in the presence of SNPs, porosity decreases from 22 to 25%, while, in presence of SF, it was from 11 to 16% compared to control in unexposed specimens. However, in the case of carbonated specimens, the porosity reduces significantly in control and SF-incorporated specimens compared to unexposed samples. The results show that the reduction in porosity in carbonated control samples was in the range of 57–73%, showing a very high rate of carbonation compare to unexposed control specimens. In cases of SF-incorporated specimens exposed to carbonation, the reduction in porosity was in the range of 27–62%; however, in the case SNPs, the reduction in porosity was almost

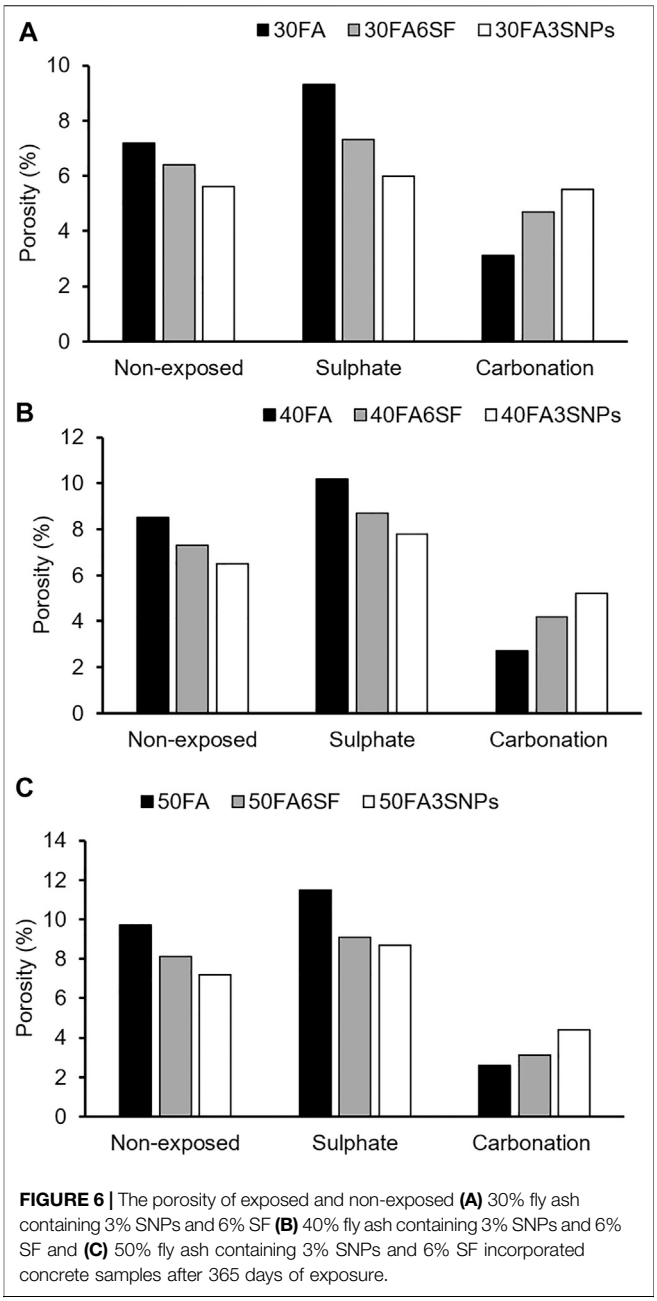

FIGURE 6 | The porosity of exposed and non-exposed **(A)** 30% fly ash containing 3% SNPs and 6% SF **(B)** 40% fly ash containing 3% SNPs and 6% SF and **(C)** 50% fly ash containing 3% SNPs and 6% SF incorporated concrete samples after 365 days of exposure.

negligible in the 30FA mix, 20% in 40FA, and 38% in the 50FA mix, exhibiting a slower rate of carbonation. Furthermore, the effect of sulphate attack on porosity was measured and results show that porosity increases in this case. In the case of control specimens, porosity increases in the range of 19–29%, while in presence of SF, the reduction was in the range of 12–20% and with SNPs, it was only in the range of 7–20% as compared to respective unexposed specimens.

XRD and TGA Analysis

The quantitative data acquired from TGA gives the information of unhydrated and hydrated products. **Figure 7** represents the CH and $CaCO_3$ content in the concrete samples exposed to a

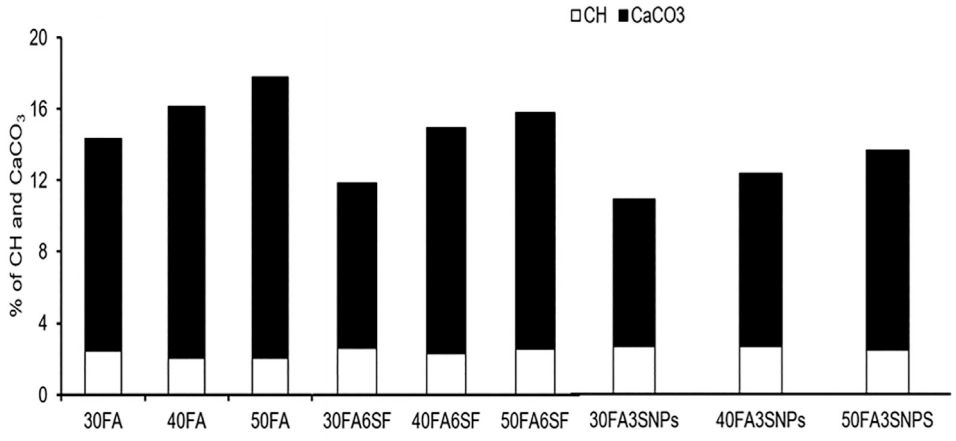

FIGURE 7 | Quantification of CH and $CaCO_3$ content in 30%, 40%, and 50% of fly ash containing 3% SNPs and 6% SF mixes by thermogravimetric analysis after 365 days of exposure.

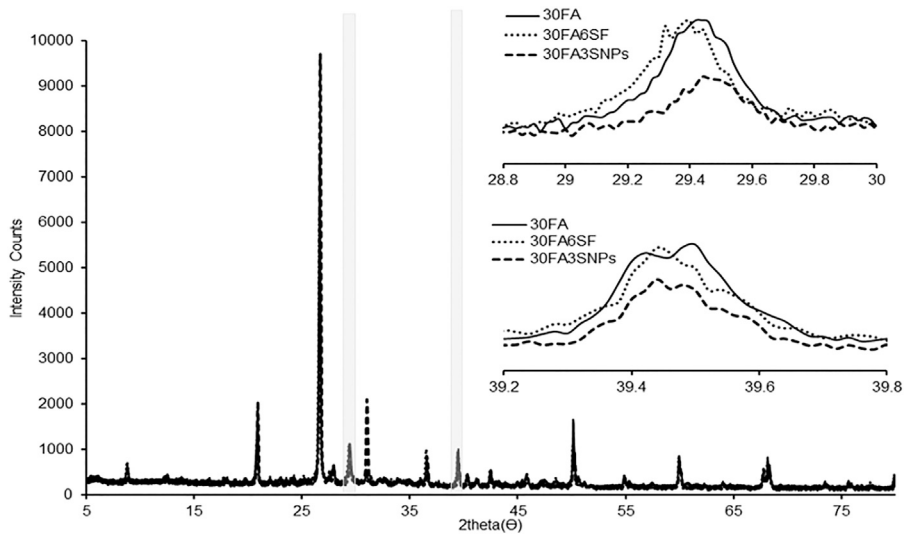

FIGURE 8 | X-ray curve of 30% fly ash containing 3% SNPs and 6% SF mixes after 365 days of exposure.

carbonated environment. The results show that as the FA content increases in the cementitious system, CH content reduced because CH is only produced by cement hydration. From the results, it is also observed that SNP- and SF-incorporated specimens show higher amounts of CH than that the control, which indicates that concrete samples containing SNPs and SF have less carbonation attack. It is well known that, during carbonation, CH react with carbonic acid and forms $CaCO_3$; the CH content was thus higher in the SF- and SNP-incorporated mix. However, the $CaCO_3$ content was significantly higher in the control and SF-incorporated mix as compare to the SNP-incorporated mix, showing a lower rate of carbonation in the presence of SNPs. It was observed that in the 30FA mix, the reduction carbonation rate was ~26%; with SF, it was ~22%. Similarly, in the 40FA and 50FA mix, the reduction in carbonation in presence of SNPs was ~27 and 25%, while, in presence of SF, it was ~11 and 16% only. This higher rate of carbonation is responsible for the lower porosity; however, the service life of the building may be adversely affected. Furthermore, XRD results also show a similar trend of results. The intensity of calcium carbonate at $2\Theta = 29.54^{\circ}$ and 39.54° was higher in control and SF incorporated specimens as compare to SNPs incorporated specimens (**Figure 8**).

Field Emission Scanning Electron Microscope

Backscattered electron (BSE) images and energy-dispersive X-ray spectroscopy (EDX) analysis of 30FA, 30FA3SNPs, and 30FA6SF mixes are shown in **Figures 9A–C**. It is a very useful technique used to perform the hydration products, and it gives perfect information of the interfacial transition zone (ITZ) in concrete

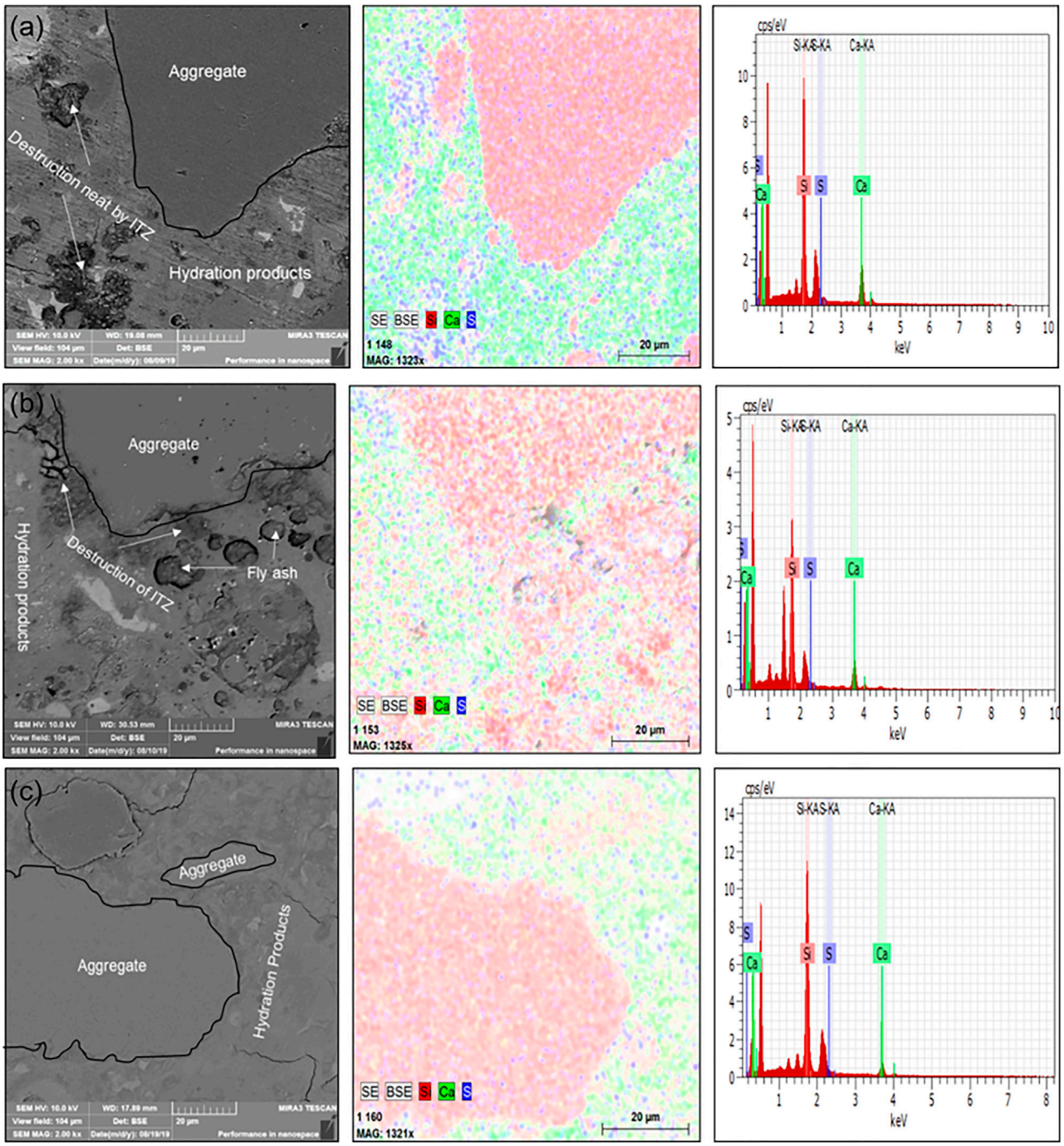

FIGURE 9 | BSE images with EDX color mapping of fly ash concrete specimens **(A)** 30FA sample **(B)** 30FA3SNPs sample **(C)** 30FA6SF sample after exposed in sulphate attack after 365 days of exposure.

microstructures. The hydration products can be recognized because of descending brightness of hydrated and unhydrated cement particles in the concrete system. In the BSE image, the dark black part considers as voids and damages, whereas the light gray part to dark gray part can be recognized as the hydration products, i.e., CH and C-S-H (Sun et al., 2018) and color mapping, which is done by EDX and also gives a lot of information about concrete samples due to the color elements as shown in **Figure 9**. The BSE image of 30FA mix after 365 days of exposure in sulphate solution can be seen in **Figure 9A**. The image clearly shows that the black pits near the ITZ in the 30FA mix are demonstrating the destruction due to the sulphate attack, which is destroying the ITZ, and it is clearly seen to break the hydration product near ITZ. The color mapping is also supported

to the BSE image, in which it is being cleared that the concentration of sulphate is more visible in the black pit, which shows that the pits are being caused due to the sulphate attack, while the SNPs sample has a lot of dance microstructure as compared to the control sample (**Figure 9B**). However, in the presence of SF, significant destruction is observed (**Figure 9C**). It has already been established that in the presence of SNPs, there is a dance microstructure of concrete and after 365 days exposed in sulphate solution, signs of breakdown of the concrete microstructure have started. TGA results are also supporting these results in which it is clear that after exposure to a sulphate solution, the CH and C-S-H start to break down. Similarly, the 30FA6SF mix image is also doing the same show that the hydration products are gradually breaking down due to the sulphate attack; because of this, cracks come appear in the concrete, and ITZ becomes weak (Tang et al., 2015).

CONCLUSION

The work carried out in the present paper is majorly focused on the durability studies of SNPs incorporated FA concrete. Durability properties i.e. sulphate attack, carbonation, and mechanical parameters were evaluated in this study and the significant observations are as follows:

1 After being exposed to carbonation, the SNP-incorporated FA concrete mix shows negligible enhancement in terms of compressive, flexural, and split tensile strength, which shows the low impact of carbonation on the SNP mix as compared to the control and SF-incorporated mix, while sulphate-exposed samples also do not demonstrate enough deficiency in strength, which is not the considerable reduction in strength.
2 Carbonation depth results confirm that, in the presence of SNPs, reduction in carbonation depth was ~57, ~32, and ~32% as compared to control after 365 days of exposure, whereas SF mixes showed ~25, ~28, and ~24% reduction only. Sulphate attack results show that reduction in sulphate ion concentration was significantly high in SNPs containing mixes as compared to control and SF concrete mixes after 365 days of exposure.
3 The TGA results show that after exposure to sulphate solution, SNPs also started the breakdown of CH and C-S-H, which was the same as the control and SF mix. In terms of the SNPs mix, due to the low effect of the sulphate attack, CH and C-S-H broke down slowly compared to the control and SF mix. BSE images also supported the TGA results since the BSE image clearly showed black pits near the ITZ, which showed the destruction of the microstructure.

The incorporation of SNPs into concrete resulted in the enhancement of durability properties of concrete; in addition to this, the performance of SNP-incorporated concrete is significantly better than that of control specimens.

DATA AVAILABILITY STATEMENT

The raw data supporting the conclusion of this article will be made available by the authors, without undue reservation.

AUTHOR CONTRIBUTIONS

Conceptualization, data curation, methodology: DA, US, and LPS; data analysis and data interpretation: DA, US, and LPS; supervision and guidance: LPS and RS; writing, reading, and approving the final manuscript: All authors.

ACKNOWLEDGMENTS

Authors are thankful to DST, New Delhi, India, for financial support through BRICS Project (DST/IMRCD/BRICS/PilotCall1/Loop/2017(G)).

REFERENCES

ACI Committee 318 (2014). Building Code Requirements for Structural Concrete (ACI 318-14) Commentary on Building Code Requirements for Structural Concrete (ACI 318R-14) An ACI Standard and Report.

ASTM C496-11, (2003). Standard Test Method for Splitting Tensile Strength of Cylindrical Concrete Specimens.

ASTM-C642, (2015). Standard Test Method for Density , Absorption , and Voids in Hardened Concrete 1.

Basheer, L., Kropp, J., and Cleland, D. J. (2001). Assessment of the Durability of Concrete from its Permeation Properties: a Review. *Construction building Mater.* 15 (2-3), 93–103. doi:10.1016/s0950-0618(00)00058-1

Chindaprasirt, P., and Rukzon, S. (2008). Strength, Porosity and Corrosion Resistance of Ternary Blend Portland Cement, Rice Husk Ash and Fly Ash Mortar. *Construction Building Mater.* 22, 1601–1606. doi:10.1016/j.conbuildmat.2007.06.010

Dananjayan, R. R. T., Kandasamy, P., and Andimuthu, R. (2016). Direct Mineral Carbonation of Coal FA for CO2 Sequestration. *J. Clean. Prod.* 112, 4173–4182. doi:10.1016/j.jclepro.2015.05.145

Demis, S., Efstathiou, M. P., and Papadakis, V. G. (2014). Computer-aided Modeling of Concrete Service Life. *Cement and Concrete Composites* 47, 9–18. doi:10.1016/j.cemconcomp.2013.11.004

Du, H., Du, S., and Liu, X. (2014). Durability Performances of Concrete with Nano-Silica. *Construction Building Mater.* 73, 705–712. doi:10.1016/j.conbuildmat.2014.10.014

El-Hachem, R., Rozière, E., Grondin, F., and Loukili, A. (2012). New Procedure to Investigate External Sulphate Attack on Cementitious Materials. *Cement and Concrete Composites* 34, 357–364. doi:10.1016/j.cemconcomp.2011.11.010

Embong, R., Kusbiantoro, A., Shafiq, N., and Nuruddin, M. F. (2016). Strength and Microstructural Properties of Fly Ash Based Geopolymer Concrete Containing High-Calcium and Water-Absorptive Aggregate. *J. Clean. Prod.* 112, 816–822. doi:10.1016/j.jclepro.2015.06.058

Gehlen, C.RILEM CPC 18 (2011). Measurement of Hardened Concrete Carbonation Depth, RILEM Tech. *Comm. TDC*, 1–11. doi:10.1617/2351580117.026

Guterres, A. (2017). *The Sustainable Development Goals Report*. New York: United Nations, 1–64.

Heikal, M., Helmy, I. M., Awad, S., and Ibrahim, N. S. (2020). Performance of Silica-Nano-Particles on the Physicochemical, and Microscopic Characteristics of Blended and Composite Cement. *Ceramics–Silikáty* 64 (3), 320–337. doi:10.13168/cs.2020.0021

Holland, T.C. (2005). Silica fume user's manual. Federal Highway Administration.

Hou, P., Kawashima, S., Kong, D., Corr, D. J., Qian, J., and Shah, S. P. (2013). Modification Effects of Colloidal nanoSiO2 on Cement Hydration and its Gel

Property. *Composites B: Eng.* 45, 440–448. doi:10.1016/j.compositesb.2012.05.056

Hou, P., Qian, J., Cheng, X., and Shah, S. P. (2014). Effects of the Pozzolanic Reactivity of Nano SiO_2 on Cement-Based Materials. *Cem. Concr. Compos.* 55, 250–258. doi:10.1016/j.cemconcomp.2014.09.014

IS-10086, (1982). Specification for moulds for use in tests of cement and concrete.

IS-3812, (2013). Specifications for Pulverized fuel ash. Indian Stand.

IS-383, (1970). Specification for coarse and fine aggragates from natural sources for concrete. Standard 1–24.

IS-4032, (1985). Method of chemical analysis of hydraulic cement. Indian Stand.

IS-456, (2000). Plain and reinforced concrete.

IS-516, (1959). Method of Tests for Strength of Concrete. Indian Stand.

IS-8112, (1989). OPC 43 grade ordinary portland cement - specification.

IS-9130, (1999). Concrete admixture- specifications.

Kawashima, S., Hou, P., Corr, D. J., and Shah, S. P. (2013). Modification of Cement-Based Materials with Nanoparticles. *Cement and Concrete Composites* 36, 8–15. doi:10.1016/j.cemconcomp.2012.06.012

Lam, L., Wong, Y. L., and Poon, C. S. (2000). Degree of Hydration and Gel/space Ratio of High-Volume Fly Ash/cement Systems. *Cement concrete Res.* 30 (5), 747–756. doi:10.1016/s0008-8846(00)00213-1

Malhotra, V. M. (1990). Durability of Concrete Incorporating High-Volume of Low-Calcium (ASTM Class F) Fly Ash. *Cement and Concrete Composites* 12 (4), 271–277. doi:10.1016/0958-9465(90)90006-j

Mazloom, M., Ramezanianpour, A. A., and Brooks, J. J. (2004). Effect of Silica Fume on Mechanical Properties of High-Strength Concrete. *Cement and Concrete Composites* 26, 347–357. doi:10.1016/s0958-9465(03)00017-9

McCarthy, M., and Dhir, R. (2005). Development of High Volume Fly Ash Cements for Use in Concrete Construction. *Fuel* 84 (11), 1423–1432. doi:10.1016/j.fuel.2004.08.029

Mo, Z., Gao, X., and Su, A. (2021). Mechanical Performances and Microstructures of Metakaolin Contained UHPC Matrix under Steam Curing Conditions. *Construction Building Mater.* 268, 121112. doi:10.1016/j.conbuildmat.2020.121112

Mukharjee, B. B., and Barai, S. V. (2014). Influence of Nano-Silica on the Properties of Recycled Aggregate Concrete. *Construction Building Mater.* 55, 29–37. doi:10.1016/j.conbuildmat.2014.01.003

Neville, A. M. (2011). *Properties of Concrete*. London, United Kingdom: Trans-Atlantic Publications, Inc.

Nili, M., and Ehsani, A. (2015). Investigating the Effect of the Cement Paste and Transition Zone on Strength Development of Concrete Containing Nanosilica and Silica Fume. *Mater. Des.* 75, 174–183. doi:10.1016/j.matdes.2015.03.024

Ohga, H., and Nagataki, S. (1989). Prediction of Carbonation Depth of Concrete with FA . FA , Silica Fume, Slag, Nat. Pozzolans Concr. ACI SP-114. *Am. Concr. Inst.* 1, 275–294. doi:10.14359/1980

Palla, R., Karade, S. R., Mishra, G., Sharma, U., and Singh, L. P. (2017). High Strength Sustainable Concrete Using Silica Nanoparticles. *Construction Building Mater.* 138, 285–295. doi:10.1016/j.conbuildmat.2017.01.129

Pereira, C. F., Luna, Y., Querol, X., Antenucci, D., and Vale, J. (2009). Waste Stabilization/solidification of an Electric Arc Furnace Dust Using FA -based Geopolymers. *Fuel* 88 (7), 1185–1193. doi:10.1016/j.fuel.2008.01.021

RameshKumar, G. B., and Muzammil, V. M. (2020). Fly ash in concrete using sea water–A review. *Mater. Today: Proc.* 22, 890–893. doi:10.1016/j.matpr.2019.11.097

Rattanachu, P., Toolkasikorn, P., Tangchirapat, W., Chindaprasirt, P., and Jaturapitakkul, C. (2020). Performance of Recycled Aggregate Concrete with Rice Husk Ash as Cement Binder. *Cement and Concrete Composites* 108, 103533. doi:10.1016/j.cemconcomp.2020.103533

Şahmaran, M., and Li, V. C. (2009). Durability Properties of Micro-cracked ECC Containing High Volumes FA. *Cement Concrete Res.* 39 (11), 1033–1043. doi:10.1016/j.cemconres.2009.07.009

Sakai, E., Miyahara, S., Ohsawa, S., Lee, S.-H., and Daimon, M. (2005). Hydration of Fly Ash Cement. *Cement Concrete Res.* 35 (6), 1135–1140. doi:10.1016/j.cemconres.2004.09.008

Salemi, N., and Behfarnia, K. (2013). Effect of Nano-Particles on Durability of Fiber-Reinforced Concrete Pavement. *Construction Building Mater.* 48, 934–941. doi:10.1016/j.conbuildmat.2013.07.037

Sanchez, F., and Sobolev, K. (2010). Nanotechnology in Concrete - A Review. *Construction Building Mater.* 24, 2060–2071. doi:10.1016/j.conbuildmat.2010.03.014

Shaikh, F. U. A., and Supit, S. W. M. (2015). Compressive Strength and Durability Properties of High Volume Fly Ash (HVFA) Concretes Containing Ultrafine Fly Ash (UFFA). *Construction Building Mater.* 82, 192–205. doi:10.1016/j.conbuildmat.2015.02.068

Sharkawi, A. M., Abd-elaty, M. A., and Khalifa, O. H. (2018). Synergistic Influence of Micro-nano Silica Mixture on Durability Performance of Cementious Materials. *Construction Building Mater.* 164, 579–588. doi:10.1016/j.conbuildmat.2018.01.013

Simatupang, P. H., Andreas, A., and Nugraha, A. (2019). The Long-Term Effects of Nano-Silica on Concrete. *IOP Conf. Ser. Mater. Sci. Eng.* 508, 12–38. doi:10.1088/1757-899x/508/1/012038

Singh, L. P., Ali, D., and Sharma, U. (2016). Studies on Optimization of Silica Nanoparticles Dosage in Cementitious System. *Cement and Concrete Composites* 70, 60–68. doi:10.1016/j.cemconcomp.2016.03.006

Singh, L. P., Ali, D., Tyagi, I., Sharma, U., Singh, R., and Hou, P. (2019). Durability Studies of Nano-Engineered Fly Ash Concrete. *Construction Building Mater.* 194, 205–215. doi:10.1016/j.conbuildmat.2018.11.022

Singh, L. P., Bhattacharyya, S. K., Shah, S. P., Mishra, G., Ahalawat, S., and Sharma, U. (2015). Studies on Early Stage Hydration of Tricalcium Silicate Incorporating Silica Nanoparticles: Part I. *Construction Building Mater.* 74, 278–286. doi:10.1016/j.conbuildmat.2014.08.046

Sobolev, K., and Shah, S. P. (2008). *Nanotechnology of Concrete: Recent Developments and Future Perspectives* Editors, in: American Concrete Institute.

Sobolev, K. (2015). Nanotechnology and Nanoengineering. *Nanotechnol. Constr.*, 3–13. doi:10.1007/978-3-319-17088-6_1

Sun, D., Wu, K., Shi, H., Zhang, L., and Zhang, L. (2018). Effect of Interfacial Transition Zone on the Transport of Sulfate Ions in Concrete. *Construction Building Mater.* 192, 28–37. doi:10.1016/j.conbuildmat.2018.10.140

Ta, V.-L., Bonnet, S., Senga Kiesse, T., and Ventura, A. (2016). A New Meta-Model to Calculate Carbonation Front Depth within Concrete Structures. *Construction Building Mater.* 129, 172–181. doi:10.1016/j.conbuildmat.2016.10.103

Taha, A. A. (2019). Performance of high-volume FA self-compacting concrete exposed to external sulfate attack.

Tang, S. W., Yao, Y., Andrade, C., and Li, Z. J. (2015). Recent Durability Studies on Concrete Structure. *Cement Concrete Res.* 78, 143–154. doi:10.1016/j.cemconres.2015.05.021

Teixeira, E. R., Mateus, R., Camões, A. F., Bragança, L., and Branco, F. G. (2016). Comparative Environmental Life-Cycle Analysis of Concretes Using Biomass and Coal Fly Ashes as Partial Cement Replacement Material. *J. Clean. Prod.* 112, 2221–2230. doi:10.1016/j.jclepro.2015.09.124

Xiao, J.-Z., Li, J.-B., and Zhang, C. (2007). On Relationships between the Mechanical Properties of Recycled Aggregate Concrete: An Overview. *Mater. Struct.* 39, 655–664. doi:10.1617/s11527-006-9093-0

Zhang, J., Chen, T., and Gao, X. (2021). Incorporation of Self-Ignited Coal Gangue in Steam Cured Precast Concrete. *J. Clean. Prod.* 292, 126004. doi:10.1016/j.jclepro.2021.126004

Conflict of Interest: The authors declare that the research was conducted in the absence of any commercial or financial relationships that could be construed as a potential conflict of interest.